Molecular Therapy
Nucleic Acids
Original Article

Novel Role for miR-1290 in Host Species Specificity of Influenza A Virus

Sheng-Yu Huang,[1,2] Chih-Heng Huang,[2,3,4] Chi-Jene Chen,[2] Ting-Wen Chen,[5,6] Chun-Yuan Lin,[2,7] Yueh-Te Lin,[2,7,8] Shu-Ming Kuo,[2] Chung-Guei Huang,[1,2,8,9] Li-Ang Lee,[10,11] Yi-Hsiang Chen,[1,2] Mei-Feng Chen,[2] Rei-Lin Kuo,[1,2,8,12] and Shin-Ru Shih[2,8,9,13,14,15]

[1]Graduate Institute of Biomedical Science, Division of Biotechnology, College of Medicine, Chang Gung University, Taoyuan 33302, Taiwan; [2]Research Center for Emerging Viral Infections, College of Medicine, Chang Gung University, Taoyuan 33302, Taiwan; [3]The Institute of Microbiology and Immunology, National Defense Medical Center, Taipei 11490, Taiwan; [4]The Institute of Preventive Medicine, National Defense Medical Center, Taipei 11490, Taiwan; [5]Institute of Bioinformatics and Systems Biology, National Chiao Tung University, Hsinchu 30068, Taiwan; [6]Department of Biological Science and Technology, National Chiao Tung University, Hsinchu, 30068, Taiwan; [7]Department of Computer Science and Information Engineering, College of Engineering, Chang Gung University, Taoyuan 33302, Taiwan; [8]Department of Medical Biotechnology and Laboratory Science, College of Medicine, Chang Gung University, Taoyuan 33302, Taiwan; [9]Department of Laboratory Medicine, Linkou Chang Gung Memorial Hospital, Taoyuan 33305, Taiwan; [10]Department of Otorhinolaryngology-Head and Neck Surgery, Linkou Chang Gung Memorial Hospital, Taoyuan 33305, Taiwan; [11]Faculty of Medicine, College of Medicine, Chang Gung University, Taoyuan 33302, Taiwan; [12]Department of Pediatrics, Linkou Chang Gung Memorial Hospital, Taoyuan 33302, Taiwan; [13]Research Center for Chinese Herbal Medicine, College of Human Ecology, Chang Gung University of Science and Technology, Taoyuan 33303, Taiwan; [14]Research Center for Food and Cosmetic Safety, College of Human Ecology, Chang Gung University of Science and Technology, Taoyuan 33303, Taiwan; [15]Graduate Institute of Health Industry Technology, College of Human Ecology, Chang Gung University of Science and Technology, Taoyuan 33303, Taiwan

The role of microRNA (miRNA) in influenza A virus (IAV) host species specificity is not well understood as yet. Here, we show that a host miRNA, miR-1290, is induced through the extracellular signal-regulated kinase (ERK) pathway upon IAV infection and is associated with increased viral titers in human cells and ferret animal models. miR-1290 was observed to target and reduce expression of the host vimentin gene. Vimentin binds with the PB2 subunit of influenza A virus ribonucleoprotein (vRNP), and knockdown of vimentin expression significantly increased vRNP nuclear retention and viral polymerase activity. Interestingly, miR-1290 was not detected in either chicken cells or mouse animal models, and the 3′ UTR of the chicken vimentin gene contains no binding site for miR-1290. These findings point to a host species-specific mechanism by which IAV upregulates miR-1290 to disrupt vimentin expression and retain vRNP in the nucleus, thereby enhancing viral polymerase activity and viral replication.

INTRODUCTION

The vast reservoir of influenza A virus (IAV) in aquatic birds serves as a genetic base that facilitates virus reassortment and antigenic shifts, some of which may confer on IAV strains the ability to cross species barriers and infect humans. Avian influenza A virus (AIV) typically does not replicate efficiently or cause disease in humans[1] because of differences in receptor binding affinity, thereby limiting virus host range.[2] Furthermore, the poor polymerase activity of AIV in human cells constitutes another major barrier that must be overcome for successful infection. The IAV viral ribonucleoprotein (vRNP) is known to harbor numerous host-determinant amino acid signatures,[3] which, when changed, can affect viral replication efficiency in different hosts. For example, a change from glutamate to lysine for amino acid residue 627 (E627K) in the PB2 subunit (PB2 K627-type) of an AIV vRNP is known to enhance polymerase activity, virus replication, viral transmission, and even pathogenicity and mortality in mammals.[4–7] Conversely, IAVs with an engineered PB2 E627-type vRNP demonstrate reduced polymerase activity in mammalian systems.[8,9] Statistical analysis indicates that most human IAVs are of the PB2 K627-type, whereas most AIVs are of the PB2 E627-type.[4,10] Our previous research also found that a host species-specific factor in humans, TUFM, exhibits stronger binding affinity with $PB2_{627}E$ than with $PB2_{627}K$ and can inhibit the replication of PB2 E627-type but not PB2 K627-type IAVs in human cells.[11] There is compelling evidence to show that AIV adaptation to humans is dependent on such mutations in the polymerase subunits (PB1, PB2, and PA) or viral nucleocapsid protein (NP), which can enhance interaction with mammalian-specific factors to enable efficient viral replication.[12] A better understanding of host species-specific factors that affect IAV replication is therefore important for the study of virus transmission and infectivity, but current research is centered on proteins, and little information is available regarding other types of regulatory factors.

MicroRNA (miRNA) is a short, noncoding RNA molecule that is believed to regulate at least 30% of cellular gene expression.[13,14]

Received 11 February 2019; accepted 29 April 2019;
https://doi.org/10.1016/j.omtn.2019.04.028.

Correspondence: Shin-Ru Shih, PhD, Research Center for Emerging Viral Infections, College of Medicine, College of Medicine, Chang Gung University, Taoyuan 33302, Taiwan
E-mail: srshih@mail.cgu.edu.tw

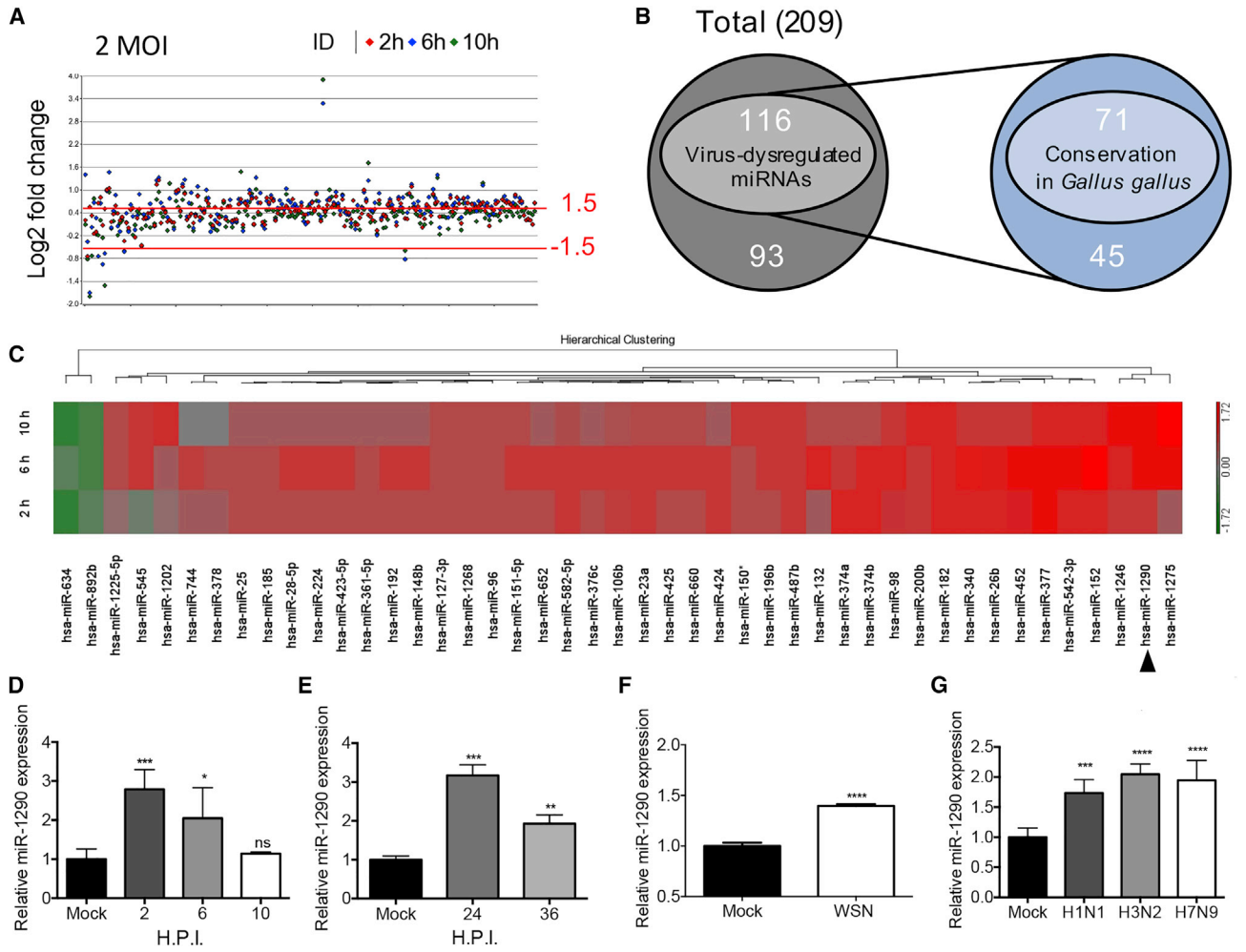

Figure 1. Dysregulation of Host Species-Specific miR-1290 Expression in IAV-Infected Human Cells

(A) A miRNA microarray analysis was performed using RNA extracts from WSN-infected A549 cells at 2, 6, and 10 h after infection with an MOI of 2 (n = 1 for each time point). The scatterplot indicates the relative expression of each identified miRNA in the WSN-infected samples, as compared with the mock-infected samples at the stated time points after infection. The y axis represents the log2-fold change of miRNA expression in the WSN-infected samples relative to the mock-infected samples. (B) A Venn diagram depicting the conservation of dysregulated miRNAs in *Gallus gallus*, analyzed by the microRNAviewer.[31] Dysregulation was determined by a threshold of a 1.5-fold change in expression relative to mock-infected controls. (C) Key miRNA expression patterns in WSN-infected A549 cells at various time points after infection. The columns correspond to expression patterns of dysregulated miRNAs relative to mock-infected samples at 2, 6, and 10 h after infection. The red and green colors respectively indicate upregulation and downregulation. MiR-1290 expression was validated in A549 cells infected with WSN (D) in a single-cycle infection at an MOI of 2 and (E) in multiple cycle infections at an MOI of 0.001. (F) Comparison of miR-1290 expression in human bronchial epithelial (NHBE) cells that were mock infected or infected with WSN at an MOI of 0.001 for 24 h. (G) Validation of miR-1290 expression in A549 cells infected with WSN (H1N1), H3N2, or H7N9 at an MOI of 0.01 for 48 h. U6 was used as an internal control, and each sample was normalized with a mock control. (D and E) Experiments were performed in triplicate and repeated at least three times. Data are presented as mean values ± SD from one representative experiment. (F and G) Data are presented as mean values ± SD from one experiment. n ≥ 3 for each sample. Error bars represent SD derived from three independent experiments. Statistical significance was determined by conducting an unpaired t test (*p < 0.05; **p < 0.01; ***p < 0.005; ****p < 0.001; ns, nonsignificant). H.P.I., hours post infection.

Individual miRNA can repress the expression of hundreds to thousands of genes through partial recognition of binding sites in the 3′ UTR of target genes.[15] Furthermore, it is now known that miRNA is involved in the replication process of both DNA and RNA viruses,[16,17] and recent studies have reported on host miRNAs that can regulate IAV replication.[18–21] Because virus replication usually involves multiple factors,[22,23] miRNAs with multi-targeting capability may serve as a more efficient and effective focus for novel antiviral drugs; moreover, it is relatively easier to develop complementary-sequence-based treatments against miRNA, as compared to protein-targeting therapies. The first miRNA-based antiviral therapy, miravirsen, is already in phase II clinical trials for the treatment of chronic hepatitis C infection.[24] However, current research has not specifically examined the role of miRNA in host species specificity.

Here, we identified a novel role for miR-1290, a host miRNA found in human and ferret lung cells, but not in mouse or chicken cells. Previously, miR-1290 expression has been reported to be upregulated in non-small cell lung cancer (NSCLC),[25] and miR-1290 has been implicated as a driver of invasiveness and proliferation in NSCLC[26–28] and lung adenocarcinoma.[29] We found that an IAV can upregulate miR-1290 expression to enhance IAV replication. When miR-1290 function was inhibited by a miR-1290 antagonist, LNA-1290, viral titers of the IAV decreased significantly in both human cells and ferret animal models. We further observed that miR-1290 can target the vimentin gene to reduce its expression. Nuclear levels of the IAV NP subunit were shown to rise in vimentin knockdown cells, and this led to significantly increased vRNP polymerase activity. Interestingly, the 3′ UTR of the chicken vimentin gene did not contain any binding site for miR-1290. These findings point to a host species-specific mechanism in which the IAV upregulates miR-1290 to interfere with vimentin expression and increase the vRNP in the host nucleus, thereby enhancing polymerase activity and viral replication.

RESULTS

Dysregulation of miR-1290 Expression Observed in IAV-Infected Human Cells

To identify miRNAs affected by IAV infection, we systematically performed miRNA microarray analysis of a human alveolar adenocarcinoma cell line, A549, which was infected with a common laboratory strain of influenza A/WSN/33(H1N1) virus (WSN). We compared miRNA expression profiles in A549 cells infected with WSN for 2, 6, and 10 h at an MOI of 2. Among 955 miRNAs on the microarray, 209 were detected in all three infected A549 samples, but most expression changes were less than 1.5-fold higher or lower when compared with analysis results from mock-infected A549 cells (Figure 1A), which is consistent with a previous report.[30] Therefore, we established a 1.5-fold expression change as a screening threshold. Further screening revealed 116 miRNAs that underwent 1.5-fold or greater expression changes at any time point following WSN infection (Figure 1B). To identify host species-specific miRNA not conserved in *Gallus* (chicken), we used microRNAviewer[31] to search for human miRNA without avian homology and subsequently found 45 miRNAs that fit this condition (Figure 1B). Comparative analysis of their expression patterns at different time points after WSN infection, using a clustered heatmap (Figure 1C), revealed that miR-1290 was strongly upregulated. We used stem-loop real-time PCR to validate miR-1290 upregulation following WSN infection and observed that for a single-cycle infection, miR-1290 expression increased by 2.8-, 2.1-, and 1.3-fold over uninfected cells at 2, 6, and 10 h after infection, respectively (Figure 1D). Moreover, for multiple-cycle infections, miR-1290 expression levels rose by 3.2- and 1.9-fold over uninfected cells at 24 and 36 h after infection, respectively (Figure 1E). To dispel concerns regarding whether such upregulation takes place only in immortalized cell lines, we repeated these experiments in normal human bronchial epithelial (NHBE) cells challenged with WSN. The results showed that miR-1290 exhibited a 1.5-fold increase in expression levels after WSN infection (Figure 1F). We proceeded to examine whether other IAV strains were similarly capable of upregulating miR-1290 expression, and our results demonstrated that levels of miR-1290 also rose significantly in cells infected with H3N2 or emerging AIV (H7N9) viruses (Figure 1G). Previous research has reported that miR-1290 is specific to humans and great apes[32] and that it is not detectable in mouse cells by *in situ* hybridization (ISH). We also used the University of California, Santa Cruz (UCSC), Genome Browser to align the miR-1290 precursor sequence across 100 vertebrate genomes and confirmed that this sequence was indeed strongly conserved across several higher primate species (Figure S1). However, to the best of our knowledge, the role of miR-1290 in IAV replication has not been reported.

miR-1290 Inhibition Disrupted IAV Replication in Human Cells and Ferrets

To further elucidate the functional impact of miR-1290 on IAV replication, we transfected a miR-1290 antagonist, LNA-1290, into A549 cells and then challenged the transfected cells with WSN virus. Real-time PCR results revealed that miR-1290 levels in transfected cells at the final post-infection time point that was tracked were about 38% that of the negative control (Figure 2A, left panel), LNA-NC, whose sequence has no homology to any known human, mouse, or rat miRNA or mRNA sequence. Corresponding viral titers examined at different time points after infection by plaque assay subsequently showed that viral titers were respectively 40% and 15% that of the negative control (LNA-NC) at 48 and 72 h after infection (Figure 2A, right panel). However, when a miR-1290 mimic alone was overexpressed in cells, at the final post-infection time point that was tracked, miR-1290 levels were upregulated 5.3-fold compared to the negative control (miR-NC; Figure 2B, left panel), and viral titers were subsequently found to be 3.8- and 1.3-fold higher than those observed in the miR-NC negative control at 48 and 72 h after infection, respectively (Figure 2B, right panel). The miR-NC negative control is a random-sequence miRNA mimic molecule that has been extensively tested in human cell lines and tissues and has been validated to have no identifiable effects on any known miRNA function. To confirm the specificity of this effect by miR-1290 on viral replication, we designed a seed sequence mutant miR-1290 mimic (sm-miR-1290) as a specific negative control. The seed sequence of the sm-miR-1290 mimic was designed to be the reverse complement of the miR-1290 sequence. Subsequent experimental results also showed that viral titers in miR-1290 overexpressed cells were 5.7- and 2.7-fold higher than this specific sm-miR-1290 negative control at 48 and 72 h after infection, respectively. We confirmed by MTT cell viability assay that both LNA-1290 and the miR-1290 mimic did not induce cell toxicity at concentrations up to 100 nM (Figure S2).

We further sought to ascertain whether LNA-1290 is capable of inhibiting IAV replication in an animal model. Although miR-1290 was previously reported to be specific to humans and great apes[32] and this was corroborated by our own genome alignment analysis (Figure S1), we nevertheless measured basal levels of miR-1290 in a variety of animal lung tissues. MiR-1290 was indeed undetectable in mouse and chicken lung tissue, but was detected in human and ferret (*Mustela putorius furo*) lung tissue (Figure 2C). Although a BLAST

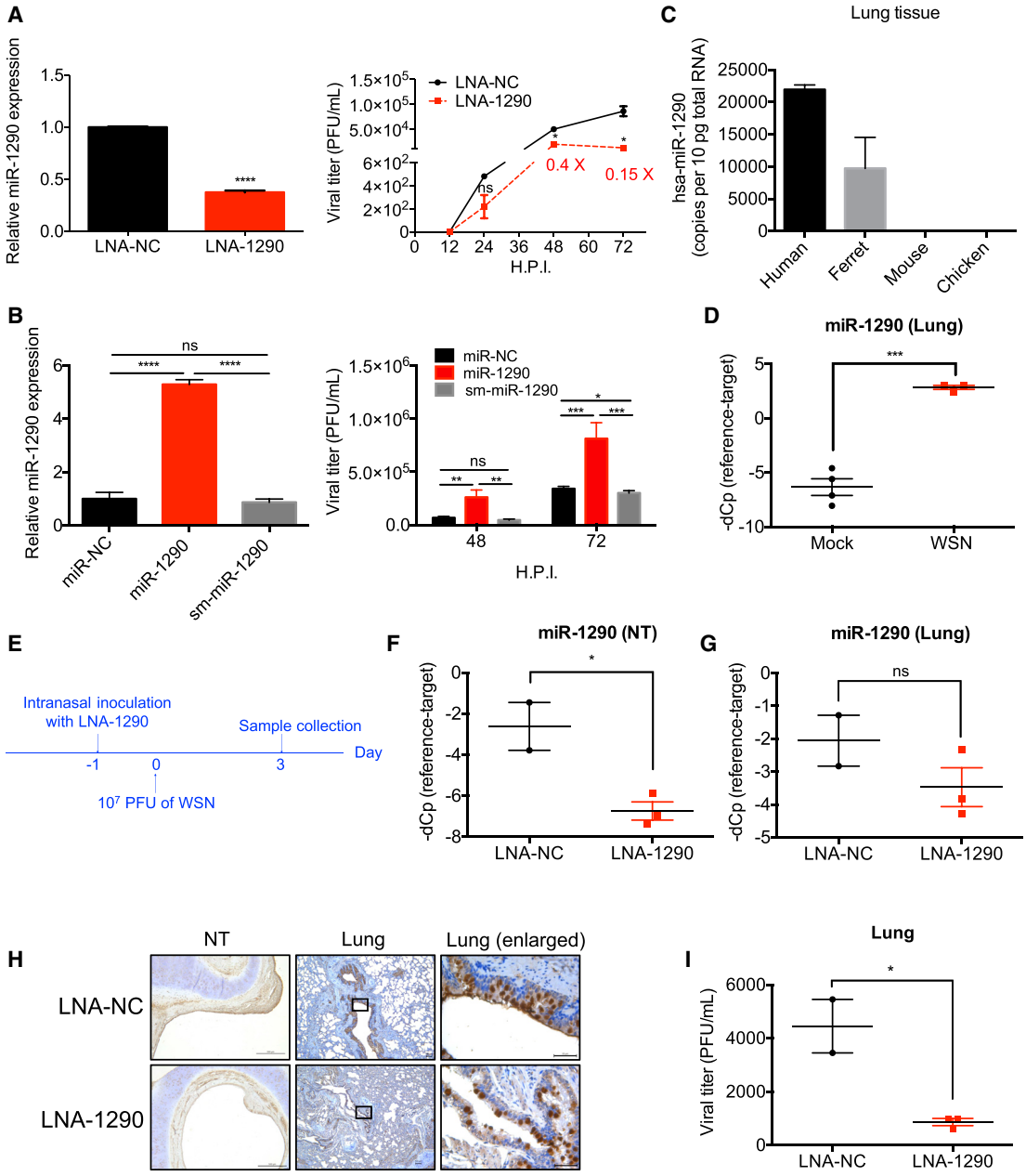

Figure 2. Inhibition of miR-1290 Reduced IAV Viral Titers in Human Cells and Ferret Models

(A and B) Comparison of miR-1290 expression levels and viral titers in (A) human A549 cells treated with a miR-1290 antagonist (LNA-1290) or a negative control (LNA-NC) or (B) human A549 cells treated with a miR-1290 mimic (miR-1290), a seed sequence mutant miR-1290 mimic (sm-miR-1290) that serves as a specific negative control, or a negative control miRNA (miR-NC). qPCR experiments (A) were performed in triplicate and repeated at least three times; for viral titer titration (B), experiments were performed in duplicate and repeated at least three times, and data are presented as mean values ± SD from one representative experiment. (C) Detected expression levels of miR-1290 in human, ferret, mouse, and chicken lung tissue. Error bars represent the SD of mean values (n = 3). (D) Real-time qPCR assessment of miR-1290 expression in mock-infected (MOCK) or WSN-infected (WSN) ferret lung tissue. (E) Schematic of the experimental setup for analysis of the relationship between miR-1290 expression and WSN viral titers in ferret models. (F) Nasal turbinate (NT) and (G) lung tissue (Lung) miR-1290 expression levels for ferrets treated with a miR-1290 antagonist (LNA-1290) or a negative control (LNA-NC). (H) Representative immunohistochemical (IHC) staining results for IAV viral proteins in the nasal turbinate (NT) or lung tissue (Lung) derived from ferrets treated with LNA-1290 or LNA-NC (×5 magnification, ×40 magnification for the enlarged panel). (I) Viral titers in the lung tissue were detected with a plaque assay. (D, F, G, and I) Two independent experiments were conducted, and data were pooled from both experiments and are presented as mean values ± SEM. Statistical significance was determined by conducting an unpaired t test (*$p < 0.05$; **$p < 0.01$; ***$p < 0.005$; ns, nonsignificant). H.P.I., hours post infection.

search produced no alignment with the miR-1290 sequence in the MusPutFur1.0 draft genome downloaded from Ensembl, we suspect that this may be due to the incompleteness of the ferret genome sequence currently available. MiR-1290 expression in ferret lung tissue was confirmed by real-time PCR, and sequencing results of the PCR product revealed an exact 100% match between ferret and human miR-1290. Considering that ferrets are an excellent mammalian model with a detailed record of use in studying the pathogenicity and transmissibility of human and avian IAV and can reflect many characteristics of IAV infection,[33] we elected to use ferrets to assess the effect of miR-1290 on IAV replication. We found that, at baseline, miR-1290 expression in ferret lung tissue was about half that in human cells, but miR-1290 levels similarly increased significantly after WSN infection, as compared with mock-infected controls (Figure 2D). We then treated ferrets intranasally with LNA-1290 1 day prior to WSN inoculation and collected tissue samples at 3 days after infection for analysis (Figure 2E). Real-time PCR results showed that miR-1290 expression decreased in the nasal turbinate (NT) and lung tissue of ferrets treated with LNA-1290, as compared to the negative controls (Figures 2F and 2G); viral protein levels (Figure 2H) and viral titers (Figure 2I) also fell in LNA-1290-treated ferrets compared to the negative controls. These results provide confirmation in an animal model that LNA-1290 can affect both viral protein levels and viral titers by inhibiting miR-1290 expression.

IAV-Enhanced miR-1290 Expression Downregulates Vimentin Expression

To better understand how miR-1290 acts to affect IAV replication, we designed a screening pipeline (Figure 3A) to investigate 62 potential target genes of miR-1290 that are important for IAV replication and are downregulated in response to IAV infection (Table S1). Screening results revealed that protein levels of vimentin were downregulated in miR-1290-overexpressing cells, but not in the negative controls (Figure 3B). To ensure that the regulation of miR-1290 on vimentin expression was not an artifact created by the miR-1290 mimic, the sm-miR-1290-specific negative control was used (Figure 3C, upper panel), and subsequent results showed that both mRNA and protein levels of vimentin were not downregulated in sm-miR-1290-overexpressing cells, as with the previous negative controls (Figure 3B) used. To verify the direct regulation specificity at the binding site between miR-1290 and the 3′ UTR of vimentin, we proceeded to construct a luciferase reporter vector containing the 3′ UTR from the human vimentin gene (*huVIM*), with the miR-1290 binding site located in this region included in either wild-type (huVIM-3′ UTR) or mutant (mut-huVIM-3′ UTR) form (Figure 3C). The reporter vector was co-transfected with miR-1290 into A549 cells, and reduced luciferase activity was observed in comparison to the negative controls or the sm-miR-1290-specific negative control in cells transfected with the wild-type huVIM-3′ UTR-containing vector (Figure 3C). By contrast, in cells transfected with the mutant mut-huVIM-3′ UTR-containing vector, for which the miR-1290 binding site is mutated, luciferase activity did not change in response to the increased miR-1290 levels (Figure 3C). These results indicate that miR-1290 can downregulate vimentin expression via binding to a specific site in the 3′ UTR of the human vimentin gene.

Downregulation of vimentin mRNA and protein levels was also observed in WSN-infected A549 cells (Figure 3D), and to confirm that this downregulation was indeed affected by miR-1290, instead of an IAV-induced transcription shutoff mechanism, we co-transfected cells with the wild-type hu-VIM-3′ UTR luciferase reporter vector, and either LNA-1290 or a negative control (LNA-NC). Following WSN infection, luciferase activity significantly decreased in cells transfected with LNA-NC, but remained comparable in LNA-1290-transfected cells, or even increased after infection (Figure 3E), indicating that LNA-1290 can block the inhibitory effect of miR-1290 on vimentin expression. We repeated this experiment in ferrets and observed that mRNA expression of the ferret vimentin gene (*feVIM*), which also contains a miR-1290 binding site in the 3′ UTR, similarly remained stable in LNA-1290-treated ferrets, as opposed to those treated with LNA-NC (Figure 3F).

Host Species-Specific miR-1290 Vimentin Regulation Is Absent in Chicken Cells

Vimentin is a highly conserved cytoskeleton protein, with 83.7% nucleotide similarity between the human and chicken vimentin coding sequence (CDS), and 74.6% similarity in the 3′ UTR. However, we did not observe any change in chicken vimentin mRNA levels in response to infection with IAV (Figure 4A). Upon analysis of the 3′ UTR of the chicken vimentin gene, we observed that there was no miR-1290 binding site (Figure 4B); however, to confirm the effects of miR-1290 on chVIM-3′ UTR, we also constructed luciferase reporter vectors containing either the wild-type chicken vimentin 3′ UTR sequence (chVIM-3′ UTR) or a mutated sequence that contained a miR-1290 binding site (mut-chVIM-3′ UTR). Overexpression of miR-1290, sm-miR-1290, or a negative control miRNA in chicken cells transfected with a luciferase reporter vector containing the wild-type chVIM-3′ UTR did not lead to any differences in luciferase expression, but overexpression of miR-1290 in chicken cells transfected with a luciferase reporter vector containing the mut-chVIM-3′ UTR led to a significant decrease in luciferase expression, as compared with the sm-miR-1290-specific negative control or previous miRNA negative controls (Figure 4B). These results confirm that miR-1290 can affect chicken vimentin expression if a binding site on the chVIM-3′ UTR is present, and the failure of miR-1290 to induce expression changes in the wild-type chicken vimentin gene indicates that such a binding site is likely not present in chickens, which also do not express miR-1290. We proceeded to transfect luciferase reporter vectors containing either huVIM-3′ UTR or chVIM-3′ UTR into A549 or DF-1 chicken fibroblast cells, after which cells were infected with WSN for 2, 6, or 10 h at an MOI of 2. Compared with mock-infected A549 cells, luciferase activity in cells transfected with huVIM-3′ UTR-containing vector decreased after infection; however, luciferase activity in DF-1 cells transfected with chVIM-3′ UTR-containing vector remained comparable to mock-infected controls, or even increased after infection

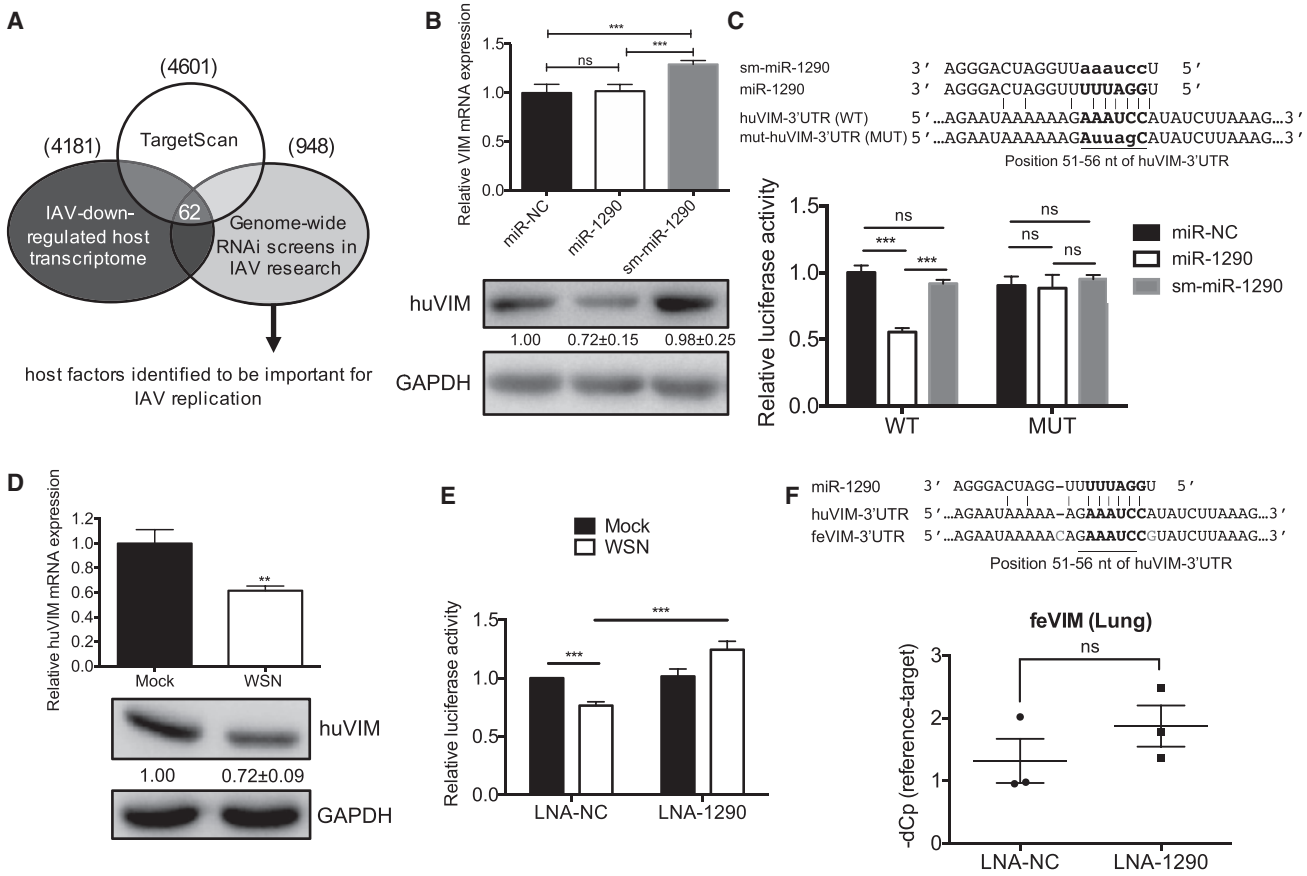

Figure 3. IAV Upregulation of miR-1290 Expression Downregulates Vimentin Expression

(A) Screening strategy used to identify miR-1290 target genes. (B) Expression levels of human vimentin gene (huVIM) mRNA and vimentin protein in miR-1290 mimic-overexpressing A549 cells. (C) The effect of miR-1290 on the luciferase activity of reporter vectors with wild-type (WT) or mutant (MUT) huVIM-3′ UTR. The putative miR-1290-binding site is located at nt 51–56 of the huVIM 3′ UTR (downstream; the first nucleotide following the stop codon is designated as +1) and is denoted in bold uppercase letters; the bold lowercase letters indicate the nucleic acid substitutions in the mutated version (mut-huVIM-3′ UTR) of the miR-1290 binding site. (D) Real-time qPCR results for huVIM mRNA expression and western blotting results for vimentin expression in A549 cells mock-infected or infected with WSN at an MOI of 2 for 6 h. Glyceraldehyde 3-phosphate dehydrogenase (GAPDH) was used as an internal control in western blotting. (E) Comparison of luciferase activity with wild-type huVIM-3′ UTR in mock- or WSN-infected A549 cells treated with a miR-1290 antagonist (LNA-1290) or control (LNA-NC). (F) Real-time qPCR results for the ferret vimentin gene (feVIM) mRNA expression in WSN-infected lung tissue treated with either LNA-1290 or LNA-NC. The putative miR-1290 binding site in the feVIM-3′ UTR is marked in bold uppercase letters and compared with the huVIM-3′ UTR. (B–E) Experiments were performed in triplicate and repeated at least three times. Data are presented as mean values ± SD from one representative experiment. (F) Two independent experiments were conducted, and data were pooled and are presented as mean values ± SD. Statistical significance was determined by conducting an unpaired t test (**$p < 0.01$; ***$p < 0.005$; ns, nonsignificant).

(Figure 4C). This indicates that IAV-induced downregulation of vimentin is likely a host species-specific mechanism.

Vimentin Knockdown Enhances Viral Polymerase Activity by Disrupting vRNP Distribution

Previous studies have shown that vimentin can associate with IAV vRNP,[34,35] and we therefore conducted an immunoprecipitation (IP) assay to assess the binding affinity of vimentin with the PB1, PB2, PA, and NP subunits of vRNP. IP results from cells transfected with FLAG-tagged vimentin and the respective vectors expressing each vRNP subunit revealed that only the PB2 subunit was pulled down by an anti-FLAG antibody (Figure 5A); however, when FLAG-tagged vimentin was overexpressed in IAV-infected cells, the PB2, PB1, PA, and NP subunits were all pulled down by an anti-FLAG antibody (Figure 5B), indicating that vimentin can interact with vRNP through binding with the PB2 subunit. A non-vRNP protein, NS1, was used as the negative control to demonstrate the binding specificity between vimentin and the vRNP subunits (Figure 5B). We observed through confocal microscopy that NP and vimentin were colocalized around the nucleus (Figure 5C) and therefore hypothesized that the interaction between vimentin and vRNP affects vRNP translocation. To ascertain this, we co-expressed vimentin small interfering RNA (siRNA) or NC siRNA, and an IAV mini-genome in A549 cells and subsequently analyzed vRNP subunit distribution

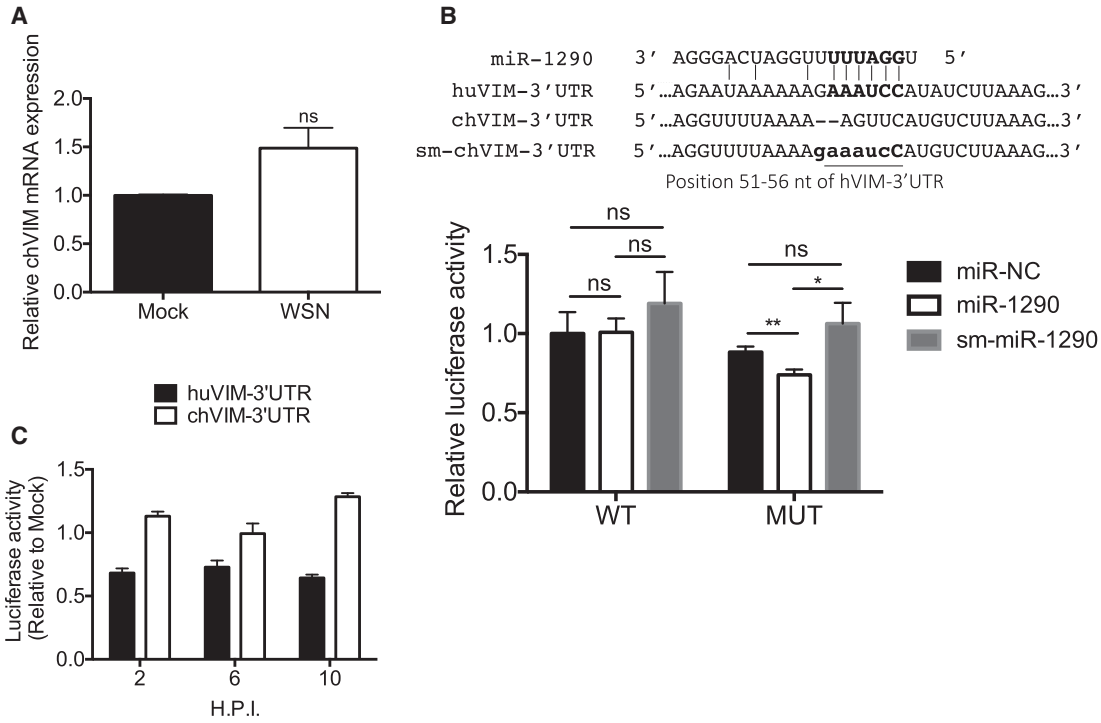

Figure 4. MiR-1290 Regulation of Vimentin was Undetectable in *Gallus gallus*

(A) Comparison of chVIM mRNA expression in chicken DF-1 cells infected with WSN at an MOI of 2 for 2 h (WSN) or mock-infected (MOCK). (B) The effect of miR-1290 on luciferase activity exhibited by reporter vectors with chicken VIM-3′ UTR (chVIM-3′ UTR) or mutant (MUT) chVIM-3′ UTR. (C) The effect of virus infections on the expression of luciferase activity with huVIM-3′ UTR or chVIM-3′ UTR assessed in WSN-infected A549 cells and WSN-infected DF-1 cells, respectively. Experiments were repeated at least three times, and data are presented as mean values ± SD from one representative experiment. Statistical significance was determined by conducting an unpaired t test (*$p < 0.05$; **$p < 0.01$; ns, nonsignificant). H.P.I., hours post infection.

in fractionated cell lysates (Figure 5D). We found that the ratio of NP subunit in the nuclear fraction of vimentin knockdown cells was higher than that in the NC siRNA. As the NP protein is one of the subunits of vRNP polymerase, to observe whether viral polymerase activity changes in vimentin knockdown cells, we co-expressed vector control (VC) or vimentin, vimentin siRNA or NC siRNA, and an IAV mini-genome in HEK293T cells to assess the impact of vimentin on vRNP activity. The results showed that vRNP activity rose in vimentin knockdown cells compared with NC siRNA controls, but when vimentin was overexpressed, no significant differences were observed in vRNP activity between cells transfected with vimentin siRNA and NC siRNA (Figure 5E). These findings suggest that vimentin may be involved in vRNP translocation, and knockdown of vimentin expression may lead to increased vRNP in the host cell nucleus, thereby enhancing viral polymerase activity.

Influenza A Virus Induces miR-1290 Expression via ERK Pathway Activation

We observed that WSN infection elevated miR-1290 expression starting from 2 h after infection, during an early stage of the viral replication cycle (Figure 1D). To explore the underlying mechanism(s), we proceeded to infect A549 cells with wild-type (WT) or UV-inactivated WSN viruses. Subsequent results showed that UV-inactivated WSN virus still increased miR-1290 levels (Figure 6A), thereby indicating that IAV-induced increases in miR-1290 expression are independent of viral RNA replication. Processes upstream of viral RNA replication, such as viral endosome uncoating or viral attachment, may also be involved in miR-1290 induction, and to understand whether the endosome-uncoated-vRNP complex is sufficient for miR-1290 induction, we treated cells with ammonium chloride (NH_4Cl) to prevent endosome fusion. Results showed that miR-1290 expression still increased in cells treated with either NH_4Cl or double-distilled water (ddH_2O) after virus infection, compared with mock-infected controls (Figure 6B). We further examined whether IAV-induced miR-1290 expression may occur at viral attachment, as previous studies have shown that IAV can activate the Raf/MEK/ERK signaling cascade in the early stages of viral infection.[36] We subsequently detected ERK activation at 30 min after viral infection (Figure 6C). It has been reported that the ERK1/2 can phosphorylate the transcription factor, Elk, to activate miR-1290 expression.[37] Therefore, we hypothesized that IAV attachment to host cells may activate the ERK pathway to promote miR-1290 transcription, and to confirm this, we assessed the expression of miR-1290 in cells treated with 12-O-tetradecanoylphorbol 13-acetate (TPA), an ERK activator. We found that p-ERK1/2 (phosphorylated ERK) was activated in

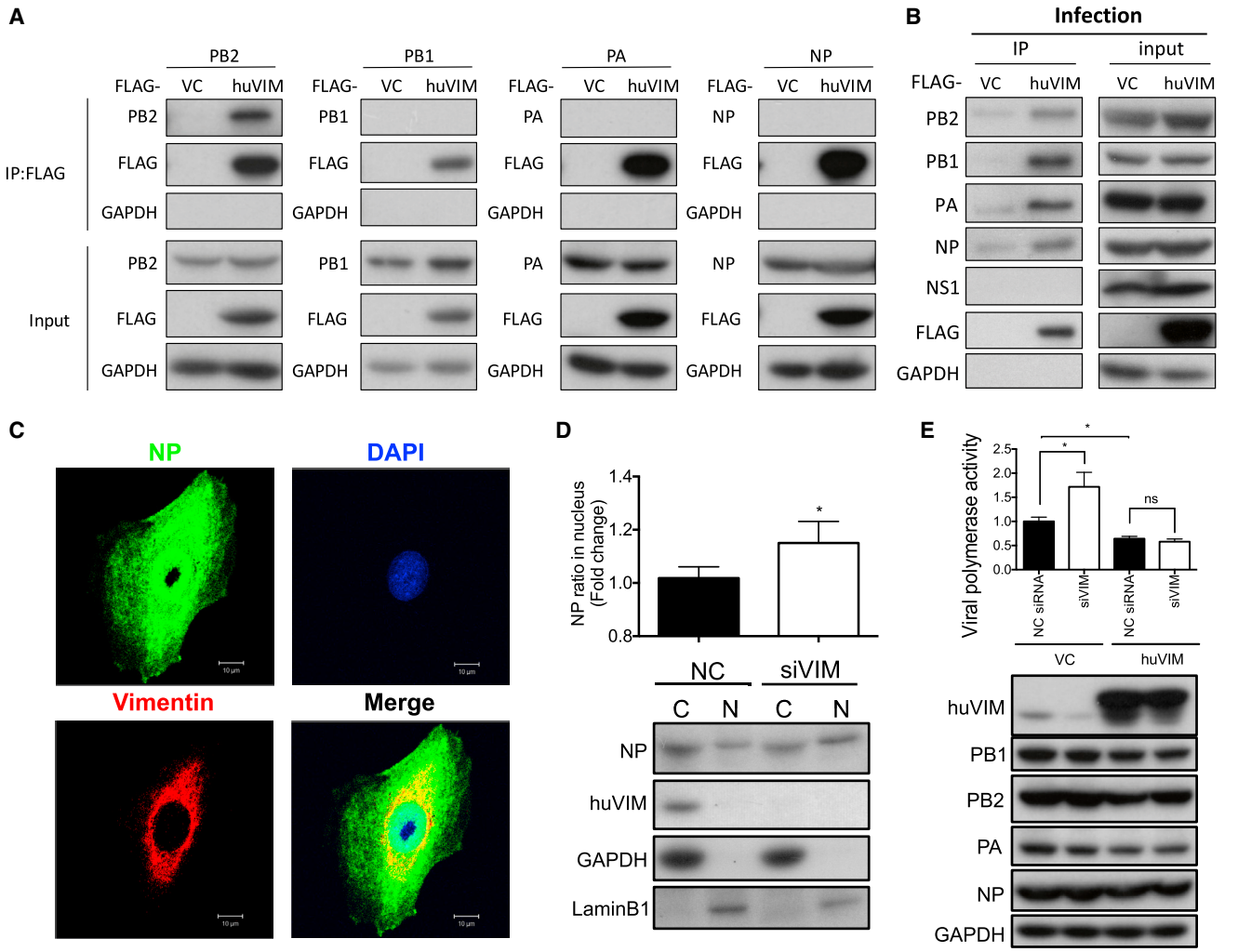

Figure 5. Vimentin Knockdown Enhances Viral Polymerase Activity by Disrupting vRNP Translocation

(A) HEK293T cells were co-transfected with constructs expressing PB2, PB1, PA, or NP, together with FLAG-tagged huVIM (huVIM) or vector control (VC). Immunoprecipitation was conducted with anti-FLAG antibodies, and precipitated proteins were detected by western blot, using the antibodies indicated at the left of each column. GAPDH was used as the control. (B) HEK293T cells infected with WSN at an MOI of 0.01 for 24 h were transfected with FLAG-tagged huVIM or VC. Immunoprecipitation was conducted with anti-FLAG antibodies, and precipitated proteins were detected by western blot, using the antibodies indicated at left. (C) Distribution of NP and vimentin in A549 cells infected with WSN at an MOI of 0.01 for 48 h after infection, using antibodies directed against vimentin (red) and NP (green). (A–C) Experiments were performed at least three times. Data are presented from one representative experiment. (D) A549 cells were co-transfected with negative control siRNA (NC siRNA) or vimentin siRNA (siVIM), as well as a WSN mini-replicon. Fractionated lysates were analyzed by western blot for detection of NP, vimentin, and the subcellular markers GAPDH and LaminB1. Quantitative results are presented as mean values ± SD from three independent experiments. (E) Viral polymerase activity in HEK293T cells transfected with vector control (VC) and treated with control siRNA (NC siRNA) or vimentin siRNA (siVIM) to induce vimentin knockdown, compared with HEK293T cells transfected with huVIM to rescue vimentin expression. The antibodies listed at left were used in western blotting of cell lysates. Luciferase activity assays were repeated at least three times, and data are presented as mean values ± SD from one representative experiment. Western blotting was performed at least three times. Data are presented from one representative experiment. Statistical significance was determined by conducting an unpaired t test (*$p < 0.05$; **$p < 0.01$; ns, nonsignificant). Non-structural viral protein NS1, which primarily functions to disrupt interferon production, was used as the negative control.

TPA-treated cells, and miR-1290 expression was also higher in TPA-treated cells than in DMSO-treated cells (Figure 6D), suggesting that IAV can activate ERK immediately after viral attachment to promote miR-1290 expression. In addition to WSN, we found that the PR8, pdmH1N1, and H3N2 viral strains promoted ERK activation (Figure 6E), and elevated miR-1290 expression was also detected after infection with these strains (Figure 6F), indicating that other IAV strains can also promote miR-1290 expression through ERK pathway activation.

DISCUSSION

Here, we identified an interesting host species-specific mechanism by which IAV exploits the miR-1290-vimentin regulation axis to

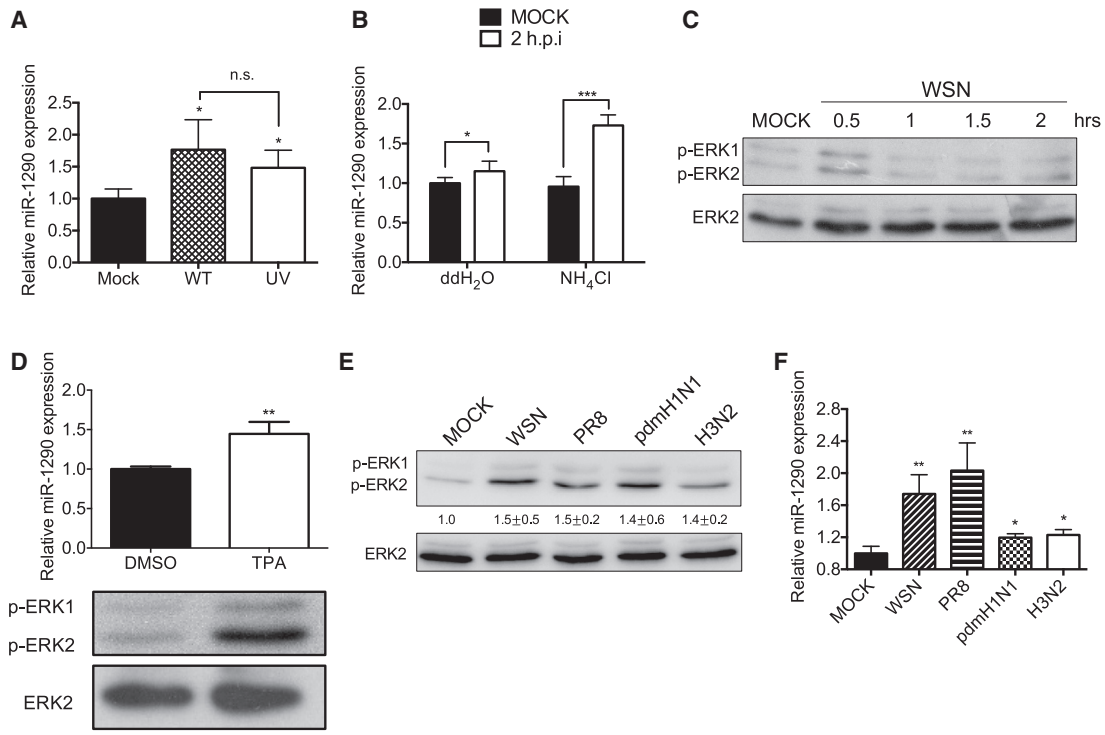

Figure 6. IAV Induces miR-1290 Expression by Activation of the ERK Pathway

(A) Comparison of miR-1290 expression in A549 cells infected with either WSN (wild type) or UV-inactivated WSN (UV) at an MOI of 2 for 2 h. (B) Comparison of miR-1290 expression in mock-infected or WSN-infected A549 cells treated with either ddH_2O or NH_4Cl. (A and B) Experiments were performed in triplicate and repeated at least three times. Data are presented as mean values ± SD from one representative experiment. (C) Validation of ERK phosphorylation in WSN-infected A549 cells. A549 cells were infected at an MOI of 5. Experiments were performed at least three times. Data are presented from one representative experiment. (D) Comparison of miR-1290 expression in DMSO- or TPA-treated A549 cells. qPCR was performed in triplicate and repeated at least three times. Data are presented as mean values ± SD from one representative experiment. Western blotting was performed at least three times. Data are presented from one representative experiment. (E) Validation of ERK phosphorylation in A549 cells infected with different IAV strains. A549 cells were infected at an MOI of 5 for 0.5 h. Western blotting was performed at least three times. Data are presented from one representative experiment. (F) Comparison of miR-1290 expression in A549 cells infected with different IAV strains at an MOI of 5 for 2 h. Experiments were performed in triplicate and repeated at least three times. Data are presented as mean values ± SD from one representative experiment. (C–E) After western blot analysis, ERK activation was analyzed with a monoclonal antibody specific to phosphorylated ERK (p-ERK). Loading levels were controlled with a polyclonal antibody against ERK2. U6 was used as an internal control, and each sample was normalized with a mock control. Error bars represent the SD derived from three independent experiments. Statistical significance was determined by conducting an unpaired t test (*$p < 0.05$; **$p < 0.01$; ***$p < 0.005$; ****$p < 0.001$; ns, nonsignificant). H.P.I., hours post infection.

promote viral replication in human lung cells and a ferret animal model. This process was not found in chicken or mouse cells, and, as more research and genome sequence data become available, the role of miR-1290 in IAV host species specificity may become clearer, as with the underlying evolutionary processes involved.

An earlier analysis of serum miRNA from patients infected with emerging AIV H7N9 found that miR-1290 was upregulated during infection,[38] and in this study, we showed that IAV infection upregulates miR-1290 expression, the result of which can benefit vRNP nuclear increase and viral replication. Interestingly, miR-1290 is located in the first intron of the *ALDH4A1* gene, and both miR-1290 and the *ALDH4A1* gene product are transcribed by the same promoter. It has been reported that *ALDH4A1* is a p53-inducible gene that is protective against cellular stresses,[39] but it is not yet known whether ALDH4A1 also plays a role in IAV infection and host species specificity. However, previous research on miR-1290 has mostly centered on its role in promoting cell proliferation and invasiveness of lung cancer,[26–29] and cellular and animal studies have shown that inhibition of miR-1290 can decrease tumor cell invasiveness and arrest xenograft tumor growth.[27,28] Considering that miR-1290 has been reported to be upregulated in NSCLC,[26] lung adenocarcinoma,[29] and other tumors, together with the fact that cancer patients appear to be at increased risk of influenza complications, further research into the impact of miR-1290 on IAV proliferation and virulence in patients with miR-1290-upregulated tumors may be warranted. The clinical effects of novel miR-1290 inhibitors, such as the LNA-1290 inhibitor described in this study, may also be worth additional investigation in both influenza and cancer.

Previous studies have also observed vimentin mRNA degradation[40] and structural alteration[41,42] during IAV infection. Interestingly, vimentin was shown to immunoprecipitate with vRNP in an earlier

study,[34] and a recent study reported that vimentin can facilitate endosome trafficking and acidification to play a critical role in IAV H5N1 infection.[43] In this study, we showed that vimentin expression is downregulated by IAV-induced miR-1290, and this leads to the nuclear enrichment of vRNP components (Figures 5C and 5D). We speculated that vimentin may interfere with vRNP import into the host cell nucleus and/or delay vRNP export from the host cell nucleus, possibly through the interaction between vimentin and vRNP that is mediated by PB2 binding. Therefore, knockdown of vimentin would reduce interference with vRNP transport, and the vRNP complex could be better retained in the nucleus during the late stage of viral replication, resulting in increased IAV vRNP activity (Figure 5E). These results do not preclude the possibility that vimentin may take on various roles at different stages of IAV infection.

Considering that the infectivity and replicative ability of IAV can differ greatly between species, it is therefore important to study the factors influencing host species specificity, particularly those with respect to humans. A robust animal model is needed to conduct such studies, and to date, mouse models have been widely employed to study the pathology of IAV. However, there are many differences between humans and mice, and mouse models may not be able to accurately reflect the human response. Our findings regarding miR-1290 represents one example of the differences between humans and mice: bioinformatic analysis (Figure S1) and real-time PCR analysis (Figure 2C) have shown that the precursor sequence of miR-1290 is absent in the mouse genome. Yelamanchili et al.[32] also verified that miR-1290 could not be detected in mouse cell lines by ISH analysis. Even though the convenience and low cost of mouse models represents a major advantage, it is possible that the use of such models may cause a promising anti-IAV therapy to be overlooked or discarded before clinical testing because of poor performance in mice. Our results suggest that ferret models may serve as an alternative or possibly better choice for studying the interaction of host factors with IAV, although further studies are likely to be needed to corroborate this.

Recently approved anti-IAV therapies primarily target viral proteins and can be broadly divided into two categories: neuraminidase inhibitors and M2 inhibitors. However, because of the high mutation rate[44,45] and reassortment capability of IAV,[46–48] drug resistance is a major issue that limits the application of these antiviral drugs.[49,50] Novel anti-viral drugs targeting host species-specific factors may represent a solution to this problem, but other side effects may emerge from these treatments, and thus more evidence regarding the use of such strategies will be needed. In this study, we observed that miR-1290 expression is enhanced upon IAV infection, and therefore we used a specific antagonist, LNA-1290, to target and block IAV-enhanced expression of miR-1290. This strategy merely reduces miR-1290 to normal pre-infection levels, and thus carries a reduced risk of side effects. We further found that intranasally applied LNA-1290 can effectively reduce IAV-induced miR-1290 overexpression in a ferret animal model, resulting in decreased viral protein levels and viral titers. These results suggest that further exploration of a therapeutic role for LNA-1290 may be worthwhile in the future.

In conclusion, our findings point to a host species-specific mechanism by which IAV utilizes miR-1290 to increase vRNP in the nucleus, thereby enhancing viral polymerase activity and viral replication. This mechanism was observed in both human cells and ferret animal models; however, miR-1290 regulation of vimentin expression was not observed in chicken cells or mouse animal models, and the 3′ UTR of the chicken vimentin gene did not contain a miR-1290 binding site. Intranasal administration of a miR-1290 antagonist, LNA-1290, subsequently reduced viral protein levels and viral titers in ferrets, suggesting that this mechanism may serve as a viable target for the future development of novel antiviral therapies. These results may also have implications for understanding how viruses can cross the species barrier and adapt to different hosts.

MATERIALS AND METHODS

Ethics Statement

The research ethics of this study were reviewed and approved by the Institutional Review Board at the Chang Gung Medical Foundation, Taoyuan, Taiwan (Approval Notices 102-4819B and 104-9560C).

Antibodies

Anti-phosphorylated-ERK (1:2,000 dilution, CST9106; Cell Signaling Technology, Danvers, MA, USA), anti-total-ERK2 (1:2,000 dilution, GTX113094; GeneTex, Irvine, CA, USA), anti-vimentin (1:1,000 dilution, sc-6260; Santa Cruz Biotechnology, Santa Cruz, CA, USA), anti-glyceraldehyde 3-phosphate dehydrogenase (GAPDH; 1:5,000 dilution, GTX100118; GeneTex), anti-actin (1:10,000 dilution, MAB1501; Millipore, Burlington, MA, USA), anti-LaminB1 (1:3,000 dilution, ab16048; Abcam, Cambridge, UK), and anti-NP (1:10,000 dilution for western blotting; 1:2,000 dilution for immunofluorescence, produced in our laboratory) antibodies were used in western blotting. Anti-influenza A (1:1,000 dilution, AB1074; Millipore) antibody was used in IHC staining.

Cells

HEK293T cells (ATCC CRL-11268), chicken fibroblast DF-1 cells (ATCC CRL-12203), and Madin-Darby canine kidney (MDCK) cells (ATCC CCL-34) were grown in DMEM (Gibco, Grand Island, NY, USA) containing 10% fetal bovine serum (FBS; Gibco). Human type II alveolar epithelial A549 cells (ATCC CCL-185) were maintained in minimum essential medium (MEM; Gibco) containing 10% FBS. NHBE cells (ATCC PCS-300-010) were grown in bronchial epithelial cell growth medium (BEGM; Lonza, Walkersville, MD, USA) containing growth factors, cytokines, and supplements. All cells were cultured at 37°C with 5% CO_2.

Viruses

The A/Taiwan/4-CGMH2/2014 (H7N9) virus was derived from Chang Gung Memorial Hospital, and the amplification and manipulation of the H7N9 virus was conducted in an accredited P3 laboratory at Chang Gung Memorial Hospital. The Pol I and Pol II plasmids of WSN virus and plasmids of A/PR8/34 were kindly provided by Dr. Robert G. Webster of the Department of Infectious Diseases, St. Jude Children's Research Hospital, Memphis, TN, USA. The whole

genome of the A/TW/3446/02 (H3N2) virus and swine-origin influenza A/Taiwan/126/2009(pdmH1N1) virus was isolated from Chang Gung Memorial Hospital and was cloned into the pHW2000 vector, as described previously.[51] The recombinant viruses were generated using 12-plasmid-based (WSN) or 8-plasmid-based (H3N2 and pdmH1N1) reverse genetic systems.[52,53]

miRNA Microarray Analysis

miRNA expression in human A549 cells was assessed with the Agilent Human miRNA Oligo Microarray R12 (Agilent Technologies), which contains probes for 866 human and 89 viral miRNAs. Signals from microarrays were analyzed with GeneSpring software version 7.3.1 (Agilent Technologies), and only miRNAs with detected flag values labeled as present were used for further analysis. Changes in miRNA expression between experimental and control samples were calculated using Partek software (Partek, St. Louis, MO, USA). The threshold used to select differentially expressed miRNAs was a greater than 1.5-fold increase or decrease in expression over controls. The data have been submitted to the NCBI GEO: GSE115069 (https://www.ncbi.nlm.nih.gov/geo/).

Real-Time Quantification of miRNA Expression by Stem-Loop RT-PCR

To synthesize cDNA from mRNA, corresponding miRNA-specific stem-loop RT primers (Table S2) and ReverTra Ace RT (Toyobo, Osaka, Japan) were used, and real-time PCR was performed using KAPA SYBR FAST qPCR Kits (Kapa Biosystems, Wilmington, MA, USA) with the corresponding primers (Table S2) on a LightCycler 480 Real-Time PCR System (Roche Applied Science, Mannheim, Germany). The specificity of the SYBR Green PCR signal was confirmed by melting-curve analysis. The PCR reaction mixture (10 μL) consisted of 5 μL of KAPA SYBR FAST qPCR solution, 3 μL of miRNA-specific anti-sense primer (Table S2), 1 μL of universal sense primers, and 1 μL of 20-fold-diluted miRNA cDNA. Cycling conditions were 95°C for 5 min, followed by 40 cycles at 95°C for 15 s, then 63°C for 32 s, and 40°C for 20 s. U6 was used as an endogenous control for normalization. Data were analyzed using the $2^{-\Delta\Delta Ct}$ method.[54]

Anti-miR and Mimic to miR-1290

To assess the cellular function of miR-1290, we used an anti-sense approach to inhibit miR-1290 function, and transfected cells with a miR-1290 mimic to increase miR-1290 expression. For these experiments, A549 cells were grown to 70% confluence and treated with anti-miR-1290 (Exiqon, Vedbaek, Denmark) or miR-1290 precursor (Ambion) using Lipofectamine 2000 (Invitrogen) according to the manufacturer's instructions.

Effect of LNA-1290 on WSN Viral Replication in Ferrets

Eight female healthy ferrets (*Mustela putorius furo*: outbred) of approximately 12 months of age, with body weights between 700 and 1,100 g and confirmed to be seronegative for antibodies against Aleutian disease virus, circulating seasonal influenza viruses, and A/WSN/33 by hemagglutination inhibition (HI) assays, were purchased from a commercial breeder. The ferrets were anesthetized by intramuscular injection (i.m.) in the hind legs with a Zoletil-xylazine cocktail prior to the administration of LNA-1290 and virus. We dissolved the lyophilized LNA-1290 (Exiqon) in Tris-EDTA (pH 8.0) to a stock concentration of 20 mg/mL, and mixed 2 mg LNA-1290 or LNA-NC control with 150 μL TransIT-TKO (Mirus Bio, Madison, WI, USA) transfection reagent and 100 μL Opti-MEM (Gibco) for each ferret. The 1 mg/kg LNA-NC or LNA-1290 complex was intranasally administered to four ferrets each, at 1 day before virus challenge. The trachea was inoculated with WSN at a dose of 10^7 plaque-forming units (PFU) in 1 mL PBS. At 3 days after infection, nasal turbinate and lung tissue were collected for further analysis.

Prediction of miR-1290 Target Genes

TargetScan was used to predict miR-1290 target genes, as described in previous research.[55] As mRNA destabilization is one of the effects that miRNA can exert on target genes, the IAV-downregulated host transcriptome was analyzed using the HumanHT-12 v4 Expression BeadChip Kit (Illumina, San Diego, CA, USA), as described in previous research.[56] The data were normalized, and calculation of the false discovery rate (FDR) was performed with Beadstudio 2.0 software (Illumina), using a customized algorithm. The genes that crossed the threshold of detection with p value ≤ 0.05, and which had a differential score p value ≤ 0.05, were considered to be differentially expressed. In addition, 948 host genes derived from RNAi-based screening assays have already been reported in the literature to be important for IAV replication.[22,23,35,57–60] Based on the integration of TargetScan predictions, IAV-downregulated transcriptome analysis results, and literature searches, 62 potential target genes were identified (Table S1). Among these, genes that were reported as part of the IAV vRNP interactome,[3,34,61–63] and for which antibodies were available in our laboratory, were subsequently selected for further study.

Luciferase Reporter Assay

For the luciferase reporter assay, the CDS of huVIM-3′ UTR and chVIM-3′ UTR derived from A549 and DF-1 cells, respectively, were cloned into the pMIR-reporter vector. huVIM-3′ UTR containing a mutant miR-1290 binding site (mut-huVIM-3′ UTR) or chicken VIM-3′ UTR containing a miR-1290 binding site (mut-chVIM-3′ UTR) was mutated from wild-type huVIM-3′ UTR or chVIM-3′ UTR by two-step RT-PCR (2× SuperRed PCR Master Mix with loading dye; BioTools, Taipei, Taiwan). At 24 or 48 h after cotransfection, the dual-luciferase-expressing cells were lysed with 50 μL passive lysis buffer (Promega, Madison, WI, USA), and firefly and *Renilla* luciferase bioluminescence was measured with a Dual-Luciferase Reporter Assay with GloMax-Multi Detection System (Promega). *Renilla* luciferase was used as an internal control.

FLAG-IP

To assess whether vimentin interacts with the IAV viral components NP, PB1, PB2, and PA (Figure 5A), HEK293T cells were respectively cotransfected with pcDNA3-PB1, pcDNA3-PB2, pcDNA3-PA, or pcDNA3-NP, and plasmids expressing FLAG-tagged human

vimentin (pFLAG-CMV2-huVIM) or a vector control (pFLAG-CMV2). After 48 h of transfection, cell lysates were collected with a FLAG Immunoprecipitation Kit (Sigma, St. Louis, MO, USA), and IP was performed using ANTI-FLAG M2 affinity gels (Sigma) and eluted using a FLAG peptide (Sigma), according to the manufacturer's protocol. Before the final wash, samples were incubated with 50 ng/μL RNaseA on ice for 30 min. The amount of input was 5% of the total IP lysates. To assess the interaction between vimentin with PB1, PB2, PA, or NP in a viral infection system (Figure 5B), HEK293T cells were transfected with plasmids expressing FLAG-tagged human vimentin (pFLAG-CMV2-huVIM) or a vector control (p FLAG-CMV2). After 24 h of transfection, the cells were infected with WSN at an MOI of 0.01 for 24 h. After 24 h of infection, cell lysates were collected and processed as described above, and the amount of input was 5% of the total IP lysates.

IFA and Confocal Microscopy

A549 cells were infected with WSN at an MOI of 0.01 for 48 h. At specific time points after infection, cells were fixed, permeabilized, stained, and analyzed as described in our previous study.[11]

Subcellular Protein Fractionation of A549 Cells Subjected to Vimentin Knockdown

A549 cells were respectively cotransfected with pcDNA3-PB1, pcDNA3-PB2, pcDNA3-PA, or pcDNA3-NP, and pol I-WSN-NS non-coding region minigenome reporter, using X-tremeGENE HP DNA Transfection Reagent (Sigma), as well as 20 nM of VIM siRNA (4390824, Silencer Select siRNAs; Thermo Fisher Scientific) or control siRNA (4390843, Silencer Negative Control No. 1 siRNA; Thermo Fisher Scientific), using Lipofectamine RNAiMAX (Invitrogen) transfection reagent according to the manufacturer's instructions. At 48 h after transfection, the cells were harvested and fractionated according to the experimental procedures described in the handbook provided along with the NE-PER Nuclear and Cytoplasmic Extraction Reagents (78833; Thermo Fisher Scientific). Approximately 60 μg of protein lysate from the cytosol fraction and lysate from the nuclear fraction at half the volume of the cytosol fraction were further used to analyze the expression of NP, vimentin, LaminB1, and GAPDH, using western blotting.

Assessing the Effect of Vimentin on vRNP Polymerase Activity

For the viral polymerase activity assay, pPolI-Luc was kindly provided by Dr. Michael M. C. Lai of the Institute of Molecular Biology, Academia Sinica, Taiwan; plasmids pcDNA-3-PB1, pcDNA-3-PB2, pcDNA-3-PA, and pcDNA-3-NP were kindly provided by Dr. Robert G. Webster of the Department of Infectious Diseases, St. Jude Children's Research Hospital, Memphis TN, USA.

To assess the effect of vimentin on IAV viral polymerase activity, HEK293T cells were cotransfected with pcDNA3-PB1, pcDNA3-PB2, pcDNA3-PA, or pcDNA3-NP, as well as pol I-WSN-NS non-coding region minigenome reporter and *Renilla* luciferase expression plasmid (pRL-TK, internal control), using Lipofectamine 2000 (Invitrogen) transfection reagent. For vimentin overexpression experiments, HEK293T cells were transfected with pFLAG-CMV-2-VIM or pFLAG-CMV-2 (vector control), using Lipofectamine 2000 (Invitrogen) transfection reagent. In vimentin knock-down experiments, HEK293T cells were transfected with 80 nM of VIM siRNA (4390824, Silencer Select siRNAs; Thermo Fisher Scientific, Waltham, MA, USA) or control siRNA (4390843, Silencer Negative Control No. 1 siRNA; Thermo Fisher Scientific), using Lipofectamine RNAiMAX (Invitrogen) transfection reagent, according to the manufacturer's instructions. At 48 h after transfection, cells were lysed with 250 μL passive lysis buffer (Promega), and firefly and *Renilla* luciferase bioluminescence was measured with the Dual-Luciferase Reporter Assay with GloMax-Multi Detection System (Promega). The protein expression of vRNP components and vimentin was analyzed by western blotting.

Expression of miR-1290 in Virus-Infected Cells Treated with NH_4Cl

A549 cells were pretreated with 40 mM NH_4Cl in serum-free MEM for 30 min before virus absorption. The cells were infected with WSN at an MOI of 2 in 40 mM NH_4Cl containing serum-free MEM for 2 h. After 2 h, cells were collected to measure miR-1290 expression using quantitative real-time PCR.

Expression of miR-1290 in Cells Treated with the ERK Activator TPA

A549 cells were treated with 100 ng/μL TPA in serum-free MEM for 30 min. After 30 min, cells were collected to measure miR-1290 expression, as well as the expression of p-ERK and total ERK, using quantitative real-time PCR and western blotting, respectively.

Statistical Analysis

The statistical analysis methods used to assess and present the results for each set of experiments are described in the figure legends.

Data and Materials Availability

Data have been submitted to the NCBI GEO: GSE115069 (https://www.ncbi.nlm.nih.gov/geo/).

SUPPLEMENTAL INFORMATION

Supplemental Information can be found online at https://doi.org/10.1016/j.omtn.2019.04.028.

AUTHOR CONTRIBUTIONS

S.-Y.H., C.-J.C., and S.-R.S. conceived and designed the study; S.-Y.H., C.-H.H., C.-J.C., Y.-T.L., S.-M.K., C.-G.H., L.-A.L., Y.-H.C., R.-L.K., and M.-F.C. conducted the experiments; T.-W.C. and C.-Y.L analyzed the data; S.-Y.H. drafted the paper; and S.-Y.H. and S.-R.S. revised the paper. All authors have read and approved the paper.

CONFLICTS OF INTEREST

Part of the findings in this study were used to support an application for a United States patent, which was subsequently granted on January 31, 2017 (Patent No. US 9,556,436 B2, with S.-R.S., C.-J.C., and S.-Y.H. as the Inventors, and Chang Gung University as the Assignee). The authors report no other competing interests.

ACKNOWLEDGMENTS

We would like to thank Dr. Robert G. Webster and Dr. Michael M. C. Lai for generously providing plasmids and Li-Zheng Tarn, DVM, for assistance with the animal work. We also thank Dr. Sung-Liang Yu, Dr. Jim-Tong Horng, and Dr. Bertrand Tan for helpful discussions related to this study. This study was supported by the Ministry of Science and Technology of Taiwan (MOST 104-2320-B-182-026-MY3 to S.-R. S.; and MOST 104-2321-B-016-002 and MOST 103-2321-B-016-006 to C.-H. H.) and Chang Gung Memorial Hospital (BMRP367 to S.-R. S.). This work was financially supported by the Research Center for Emerging Viral Infections from The Featured Areas Research Center Program within the framework of the Higher Education Sprout Project by the Ministry of Education (MOE) in Taiwan and the Ministry of Science and Technology (MOST), Taiwan (MOST 108-3017-F-182-001). The funders had no role in the study design, data collection and interpretation, or the decision to submit the study results for publication.

REFERENCES

1. Beare, A.S., and Webster, R.G. (1991). Replication of avian influenza viruses in humans. Arch. Virol. *119*, 37–42.
2. Suzuki, Y., Ito, T., Suzuki, T., Holland, R.E., Jr., Chambers, T.M., Kiso, M., Ishida, H., and Kawaoka, Y. (2000). Sialic acid species as a determinant of the host range of influenza A viruses. J. Virol. *74*, 11825–11831.
3. Naffakh, N., Tomoiu, A., Rameix-Welti, M.A., and van der Werf, S. (2008). Host restriction of avian influenza viruses at the level of the ribonucleoproteins. Annu. Rev. Microbiol. *62*, 403–424.
4. Subbarao, E.K., London, W., and Murphy, B.R. (1993). A single amino acid in the PB2 gene of influenza A virus is a determinant of host range. J. Virol. *67*, 1761–1764.
5. Steel, J., Lowen, A.C., Mubareka, S., and Palese, P. (2009). Transmission of influenza virus in a mammalian host is increased by PB2 amino acids 627K or 627E/701N. PLoS Pathog. *5*, e1000252.
6. Fornek, J.L., Gillim-Ross, L., Santos, C., Carter, V., Ward, J.M., Cheng, L.I., Proll, S., Katze, M.G., and Subbarao, K. (2009). A single-amino-acid substitution in a polymerase protein of an H5N1 influenza virus is associated with systemic infection and impaired T-cell activation in mice. J. Virol. *83*, 11102–11115.
7. Li, J., Ishaq, M., Prudence, M., Xi, X., Hu, T., Liu, Q., and Guo, D. (2009). Single mutation at the amino acid position 627 of PB2 that leads to increased virulence of an H5N1 avian influenza virus during adaptation in mice can be compensated by multiple mutations at other sites of PB2. Virus Res. *144*, 123–129.
8. Mehle, A., and Doudna, J.A. (2008). An inhibitory activity in human cells restricts the function of an avian-like influenza virus polymerase. Cell Host Microbe *4*, 111–122.
9. Moncorgé, O., Mura, M., and Barclay, W.S. (2010). Evidence for avian and human host cell factors that affect the activity of influenza virus polymerase. J. Virol. *84*, 9978–9986.
10. Chen, G.W., Chang, S.C., Mok, C.K., Lo, Y.L., Kung, Y.N., Huang, J.H., Shih, Y.H., Wang, J.Y., Chiang, C., Chen, C.J., and Shih, S.R. (2006). Genomic signatures of human versus avian influenza A viruses. Emerg. Infect. Dis. *12*, 1353–1360.
11. Kuo, S.M., Chen, C.J., Chang, S.C., Liu, T.J., Chen, Y.H., Huang, S.Y., and Shih, S.R. (2017). Inhibition of avian influenza A virus replication in human cells by host restriction factor tufm is correlated with autophagy. MBio *8*, e00481-17.
12. Mänz, B., Schwemmle, M., and Brunotte, L. (2013). Adaptation of avian influenza A virus polymerase in mammals to overcome the host species barrier. J. Virol. *87*, 7200–7209.
13. Lewis, B.P., Burge, C.B., and Bartel, D.P. (2005). Conserved seed pairing, often flanked by adenosines, indicates that thousands of human genes are microRNA targets. Cell *120*, 15–20.
14. Friedman, R.C., Farh, K.K., Burge, C.B., and Bartel, D.P. (2009). Most mammalian mRNAs are conserved targets of microRNAs. Genome Res. *19*, 92–105.
15. Huntzinger, E., and Izaurralde, E. (2011). Gene silencing by microRNAs: contributions of translational repression and mRNA decay. Nat. Rev. Genet. *12*, 99–110.
16. Voinnet, O. (2005). Induction and suppression of RNA silencing: insights from viral infections. Nat. Rev. Genet. *6*, 206–220.
17. Gottwein, E., and Cullen, B.R. (2008). Viral and cellular microRNAs as determinants of viral pathogenesis and immunity. Cell Host Microbe *3*, 375–387.
18. Bakre, A., Andersen, L.E., Meliopoulos, V., Coleman, K., Yan, X., Brooks, P., Crabtree, J., Tompkins, S.M., and Tripp, R.A. (2013). Identification of host kinase genes required for influenza virus replication and the regulatory role of microRNAs. PLoS ONE *8*, e66796.
19. Othumpangat, S., Noti, J.D., and Beezhold, D.H. (2014). Lung epithelial cells resist influenza A infection by inducing the expression of cytochrome c oxidase VIc which is modulated by miRNA 4276. Virology *468-470*, 256–264.
20. Khongnomnan, K., Makkoch, J., Poomipak, W., Poovorawan, Y., and Payungporn, S. (2015). Human miR-3145 inhibits influenza A viruses replication by targeting and silencing viral PB1 gene. Exp. Biol. Med. (Maywood) *240*, 1630–1639.
21. Loveday, E.K., Diederich, S., Pasick, J., and Jean, F. (2015). Human microRNA-24 modulates highly pathogenic avian-origin H5N1 influenza A virus infection in A549 cells by targeting secretory pathway furin. J. Gen. Virol. *96*, 30–39.
22. Karlas, A., Machuy, N., Shin, Y., Pleissner, K.P., Artarini, A., Heuer, D., Becker, D., Khalil, H., Ogilvie, L.A., Hess, S., et al. (2010). Genome-wide RNAi screen identifies human host factors crucial for influenza virus replication. Nature *463*, 818–822.
23. König, R., Stertz, S., Zhou, Y., Inoue, A., Hoffmann, H.H., Bhattacharyya, S., Alamares, J.G., Tscherne, D.M., Ortigoza, M.B., Liang, Y., et al. (2010). Human host factors required for influenza virus replication. Nature *463*, 813–817.
24. Gebert, L.F.R., Rebhan, M.A.E., Crivelli, S.E.M., Denzler, R., Stoffel, M., and Hall, J. (2014). Miravirsen (SPC3649) can inhibit the biogenesis of miR-122. Nucleic Acids Res. *42*, 609–621.
25. Yang, C., Sun, C., Liang, X., Xie, S., Huang, J., and Li, D. (2016). Integrative analysis of microRNA and mRNA expression profiles in non-small-cell lung cancer. Cancer Gene Ther. *23*, 90–97.
26. Mo, D., Gu, B., Gong, X., Wu, L., Wang, H., Jiang, Y., Zhang, B., Zhang, M., Zhang, Y., Xu, J., and Pan, S. (2015). miR-1290 is a potential prognostic biomarker in non-small cell lung cancer. J. Thorac. Dis. *7*, 1570–1579.
27. Kim, G., An, H.J., Lee, M.J., Song, J.Y., Jeong, J.Y., Lee, J.H., and Jeong, H.C. (2016). Hsa-miR-1246 and hsa-miR-1290 are associated with stemness and invasiveness of non-small cell lung cancer. Lung Cancer *91*, 15–22.
28. Zhang, W.C., Chin, T.M., Yang, H., Nga, M.E., Lunny, D.P., Lim, E.K., Sun, L.L., Pang, Y.H., Leow, Y.N., Malusay, S.R., et al. (2016). Tumour-initiating cell-specific miR-1246 and miR-1290 expression converge to promote non-small cell lung cancer progression. Nat. Commun. *7*, 11702.
29. Xiao, X., Yang, D., Gong, X., Mo, D., Pan, S., and Xu, J. (2018). miR-1290 promotes lung adenocarcinoma cell proliferation and invasion by targeting SOCS4. Oncotarget *9*, 11977–11988.
30. Buggele, W.A., Krause, K.E., and Horvath, C.M. (2013). Small RNA profiling of influenza A virus-infected cells identifies miR-449b as a regulator of histone deacetylase 1 and interferon beta. PLoS ONE *8*, e76560.
31. Kiezun, A., Artzi, S., Modai, S., Volk, N., Isakov, O., and Shomron, N. (2012). miRviewer: a multispecies microRNA homologous viewer. BMC Res. Notes *5*, 92.
32. Yelamanchili, S.V., Morsey, B., Harrison, E.B., Rennard, D.A., Emanuel, K., Thapa, I., Bastola, D.R., and Fox, H.S. (2014). The evolutionary young miR-1290 favors mitotic exit and differentiation of human neural progenitors through altering the cell cycle proteins. Cell Death Dis. *5*, e982.
33. Oh, D.Y., and Hurt, A.C. (2016). Using the ferret as an animal model for investigating influenza antiviral effectiveness. Front. Microbiol. *7*, 80.
34. Mayer, D., Molawi, K., Martínez-Sobrido, L., Ghanem, A., Thomas, S., Baginsky, S., Grossmann, J., García-Sastre, A., and Schwemmle, M. (2007). Identification of cellular interaction partners of the influenza virus ribonucleoprotein complex and polymerase complex using proteomic-based approaches. J. Proteome Res. *6*, 672–682.
35. Watanabe, T., Kawakami, E., Shoemaker, J.E., Lopes, T.J., Matsuoka, Y., Tomita, Y., Kozuka-Hata, H., Gorai, T., Kuwahara, T., Takeda, E., et al. (2014). Influenza virus-

host interactome screen as a platform for antiviral drug development. Cell Host Microbe *16*, 795–805.

36. Marjuki, H., Gornitzky, A., Marathe, B.M., Ilyushina, N.A., Aldridge, J.R., Desai, G., Webby, R.J., and Webster, R.G. (2011). Influenza A virus-induced early activation of ERK and PI3K mediates V-ATPase-dependent intracellular pH change required for fusion. Cell. Microbiol. *13*, 587–601.

37. Zhu, Y., Jiang, Q., Lou, X., Ji, X., Wen, Z., Wu, J., Tao, H., Jiang, T., He, W., Wang, C., et al. (2012). MicroRNAs up-regulated by CagA of Helicobacter pylori induce intestinal metaplasia of gastric epithelial cells. PLoS ONE *7*, e35147.

38. Zhu, Z., Qi, Y., Ge, A., Zhu, Y., Xu, K., Ji, H., Shi, Z., Cui, L., and Zhou, M. (2014). Comprehensive characterization of serum microRNA profile in response to the emerging avian influenza A (H7N9) virus infection in humans. Viruses *6*, 1525–1539.

39. Yoon, K.A., Nakamura, Y., and Arakawa, H. (2004). Identification of ALDH4 as a p53-inducible gene and its protective role in cellular stresses. J. Hum. Genet. *49*, 134–140.

40. Beloso, A., Martínez, C., Valcárcel, J., Santarén, J.F., and Ortín, J. (1992). Degradation of cellular mRNA during influenza virus infection: its possible role in protein synthesis shutoff. J. Gen. Virol. *73*, 575–581.

41. Wheeler, J.G., Winkler, L.S., Seeds, M., Bass, D., and Abramson, J.S. (1990). Influenza A virus alters structural and biochemical functions of the neutrophil cytoskeleton. J. Leukoc. Biol. *47*, 332–343.

42. Arcangeletti, M.C., Pinardi, F., Missorini, S., De Conto, F., Conti, G., Portincasa, P., Scherrer, K., and Chezzi, C. (1997). Modification of cytoskeleton and prosome networks in relation to protein synthesis in influenza A virus-infected LLC-MK2 cells. Virus Res. *51*, 19–34.

43. Wu, W., and Panté, N. (2016). Vimentin plays a role in the release of the influenza A viral genome from endosomes. Virology *497*, 41–52.

44. Parvin, J.D., Moscona, A., Pan, W.T., Leider, J.M., and Palese, P. (1986). Measurement of the mutation rates of animal viruses: influenza A virus and poliovirus type 1. J. Virol. *59*, 377–383.

45. Nobusawa, E., and Sato, K. (2006). Comparison of the mutation rates of human influenza A and B viruses. J. Virol. *80*, 3675–3678.

46. Castrucci, M.R., Donatelli, I., Sidoli, L., Barigazzi, G., Kawaoka, Y., and Webster, R.G. (1993). Genetic reassortment between avian and human influenza A viruses in Italian pigs. Virology *193*, 503–506.

47. Zhou, N.N., Senne, D.A., Landgraf, J.S., Swenson, S.L., Erickson, G., Rossow, K., Liu, L., Yoon, Kj., Krauss, S., and Webster, R.G. (1999). Genetic reassortment of avian, swine, and human influenza A viruses in American pigs. J. Virol. *73*, 8851–8856.

48. Lu, L., Lycett, S.J., and Leigh Brown, A.J. (2014). Reassortment patterns of avian influenza virus internal segments among different subtypes. BMC Evol. Biol. *14*, 16.

49. Kelso, A., and Hurt, A.C. (2012). The ongoing battle against influenza: Drug-resistant influenza viruses: why fitness matters. Nat. Med. *18*, 1470–1471.

50. Hayden, F.G., and de Jong, M.D. (2011). Emerging influenza antiviral resistance threats. J. Infect. Dis. *203*, 6–10.

51. Neumann, G., Watanabe, T., Ito, H., Watanabe, S., Goto, H., Gao, P., Hughes, M., Perez, D.R., Donis, R., Hoffmann, E., et al. (1999). Generation of influenza A viruses entirely from cloned cDNAs. Proc. Natl. Acad. Sci. USA *96*, 9345–9350.

52. Hoffmann, E., Neumann, G., Kawaoka, Y., Hobom, G., and Webster, R.G. (2000). A DNA transfection system for generation of influenza A virus from eight plasmids. Proc. Natl. Acad. Sci. USA *97*, 6108–6113.

53. Hoffmann, E., and Webster, R.G. (2000). Unidirectional RNA polymerase I-polymerase II transcription system for the generation of influenza A virus from eight plasmids. J. Gen. Virol. *81*, 2843–2847.

54. Chhabra, R., Dubey, R., and Saini, N. (2011). Gene expression profiling indicate role of ER stress in miR-23a∼27a∼24-2 cluster induced apoptosis in HEK293T cells. RNA Biol. *8*, 648–664.

55. Agarwal, V., Bell, G.W., Nam, J.W., and Bartel, D.P. (2015). Predicting effective microRNA target sites in mammalian mRNAs. eLife *4*, e05005.

56. Hao, L., Sakurai, A., Watanabe, T., Sorensen, E., Nidom, C.A., Newton, M.A., Ahlquist, P., and Kawaoka, Y. (2008). Drosophila RNAi screen identifies host genes important for influenza virus replication. Nature *454*, 890–893.

57. Brass, A.L., Huang, I.C., Benita, Y., John, S.P., Krishnan, M.N., Feeley, E.M., Ryan, B.J., Weyer, J.L., van der Weyden, L., Fikrig, E., et al. (2009). The IFITM proteins mediate cellular resistance to influenza A H1N1 virus, West Nile virus, and dengue virus. Cell *139*, 1243–1254.

58. Shapira, S.D., Gat-Viks, I., Shum, B.O., Dricot, A., de Grace, M.M., Wu, L., Gupta, P.B., Hao, T., Silver, S.J., Root, D.E., et al. (2009). A physical and regulatory map of host-influenza interactions reveals pathways in H1N1 infection. Cell *139*, 1255–1267.

59. Su, W.C., Chen, Y.C., Tseng, C.H., Hsu, P.W., Tung, K.F., Jeng, K.S., and Lai, M.M. (2013). Pooled RNAi screen identifies ubiquitin ligase Itch as crucial for influenza A virus release from the endosome during virus entry. Proc. Natl. Acad. Sci. USA *110*, 17516–17521.

60. Cheng, Q., Pappas, V., Hallmann, A., and Miller, S.M. (2005). Hsp70A and GlsA interact as partner chaperones to regulate asymmetric division in Volvox. Dev. Biol. *286*, 537–548.

61. Dyer, M.D., Murali, T.M., and Sobral, B.W. (2008). The landscape of human proteins interacting with viruses and other pathogens. PLoS Pathog. *4*, e32.

62. Nagata, K., Kawaguchi, A., and Naito, T. (2008). Host factors for replication and transcription of the influenza virus genome. Rev. Med. Virol. *18*, 247–260.

63. Li, Y., Anderson, D.H., Liu, Q., and Zhou, Y. (2008). Mechanism of influenza A virus NS1 protein interaction with the p85β, but not the p85α, subunit of phosphatidylinositol 3-kinase (PI3K) and up-regulation of PI3K activity. J. Biol. Chem. *283*, 23397–23409.